Early stages of solute clustering in an Al-Mg-Si alloy

Meng Liu,[a,c,*] Jakub Čížek,[b] Cynthia S.T. Chang[c] and John Banhart[a,c]

[a]Technische Universität Berlin, Hardenbergstraße 36, 10623 Berlin, Germany

[b]Charles University, V Holešovičkách 2, 18000 Praha 8, Czech Republic

[c]Helmholtz-Zentrum Berlin, Hahn-Meitner-Platz 1, 14109 Berlin, Germany

The processes taking place during natural ageing (NA) of the aluminium alloy Al-0.4Mg-0.4Si (wt.%) are characterised by positron annihilation lifetime spectroscopy carried out both *in-situ* during ageing and *ex-situ* after cooling down samples to low temperatures (–180 °C to –60 °C) between NA steps. We find a pronounced dependence of positron lifetime on temperature, which is the signature of the presence of vacancy-free solute clusters in addition to vacancy-related defects. Such clusters are also found in as-quenched samples, indicating that clustering takes place already during quenching. The decomposition of positron lifetime spectra into various components allows us to apply the three-state trapping model and to determine the trapping rates into vacancy-related defects and solute clusters. By modelling the time dependence of positron data we are able to describe the natural ageing process as a gradual decrease of vacancy density associated with a pronounced increase of the density of solute clusters.

1. Introduction

Immediately after quenching aluminium alloys from the solutionising temperature to 'room temperature', normally 20 °C or below, vacancy migration and solute diffusion set in and give rise to the continuous formation and development of solute clusters. In alloys such as Al-Mg-Si, these changes lead to pronounced macroscopic effects such as a rise of electrical resistivity and hardness as well as of a decrease of positron lifetime [1-3]. Moreover the formation of such clusters influences the subsequent artificial ageing process, either positively [4] or negatively [5], which explains the interest in studies of 'room temperature' natural ageing (NA). Little is known about the phenomena during the early stages of NA.

The clusters formed at 'room temperature' have not been visualised in the transmission electron microscope. Only atom probe can make them visible, but at the earliest after ~1 h [6], which is the time the samples age during sample preparation. Therefore, atom probe can tell us only what happens after 1 h or later. In addition, the results of the various studies are partially contradictory. 70 d of NA produced co-clusters with Mg:Si ratios around 1 in one study [7,8], after 7 d of NA the Mg:Si ratio was 1.2 in another [9]. Some Mg clusters [7] or no clusters [10] were found in the 'as-quenched' state, i.e. after short NA during sample preparation. In these studies, Cu-free alloys containing about 0.75% Mg and Si were used. In a Si-rich alloy after 1 week of NA, only Si clusters were found, no Mg-Si co-clusters [11]. In Mg-rich alloys NA was found to increase the average Mg:Si ratio from 0.8 after 2.5 h of NA to 1.6 after 2.5 years of NA [12]. The Mg:Si ratio of individual clusters was found to vary from ~0.5 to > 4 while the cluster size remained almost constant between 1 week and 2.5 years of

NA with clusters containing mostly between 20 and 50 solute atoms [13]. Directly after quenching, no solute clusters were found at all [14]. Torsæter [15] confirmed the wide distributions of Mg:Si ratio for a similar alloy, but found a Mg:Si distribution centred around 1 for an alloy with low solute content. NMR spectroscopy has recently shown that an increasing amount of Mg can be detected in the clusters after 100 min of NA in Al-Mg-Si alloys [16]. In summary, it is known that clusters are formed and grow during NA, but the exact details especially for the very early stages (i.e. < 1 h) remain unknown.

Positron lifetime spectroscopy has been used to study NA in a series of Al-Mg-Si alloys directly from the onset of NA after quenching with a repetition time of measurements around 2 min [3]. It was found that the (one-component) positron lifetime evolves in four typical stages. In Al-0.4Mg-0.4Si – the alloy investigated in this work – the initial positron lifetime 2 min after quenching is around 0.240 ns, slightly lower than in a single vacancy in aluminium (~0.250 ns). After a short transient stage I of slightly increasing lifetime (only measurable at NA temperatures of 0 °C or below [17]), the lifetimes drop by more than 0.03 ns in stage II, which lasts for about 84±12 min. A possible explanation for this decrease would be a progressing loss of vacancies which causes the positrons to increasingly annihilate in the bulk matrix where they live shorter. This, however, would give rise to a measurable and increasing second lifetime component, which was not found. In contrast, the measurements reported in Ref. [3] rather gave evidence for a second component right after quenching that vanished towards the end of stage II. However, due to limited resolution of the spectrometer used this result was not considered conclusive. A second lifetime component that

vanished for longer NA has been reported in a similar alloy 5 min after quenching [18], but those measurements are not consistent with those of Ref. [3]. To explain these findings the idea was developed that a further kind of positron trap with a characteristic positron lifetime of ~0.200 ns is formed during NA and gains importance during NA. It was postulated that this component is caused by vacancy-free solute clusters of Mg and Si [3]. A reported temperature dependence of the measured positron lifetime [19] strengthened this viewpoint since only shallow positron traps such as solute clusters would show this temperature dependence but not vacancy-related traps or the bulk matrix [20]. In stage III, the positron lifetime increases again. This has been attributed to the influence of Mg that – once incorporated into the clusters – would increase the positron lifetime [3]. Stage IV is a final decrease of positron lifetime which continues for a few weeks.

The positron lifetime evolution during NA at different temperatures has been successfully modelled based on abovementioned idea, namely that there are two types of traps, one vacancy-related trap with a typical lifetime τ = 0.244 ns and another with τ ranging from 0.209 to 0.218 ns. No bulk annihilation component was assumed [16]. Although the success of this model makes the existence of two kinds of positron traps more likely, nothing is said about the nature of these traps and a direct experimental verification is still lacking.

One aim of this paper is to provide decompositions of the positron lifetime into various components to identify the various positron traps directly. For this we employ a high-resolution lifetime spectrometer. Another aim is to measure the temperature dependence of positron lifetime in various stages of natural ageing and to relate the

dependence to the results of the lifetime compositions. The final result is the identification of the processes during natural ageing.

2. Experimental

2.1 Sample preparation

A ternary aluminium alloy containing 0.4 wt.% Mg and 0.4 wt.% Si (0.45 at.% Mg and 0.38 at.% Si) was used for this study. It is the same alloy investigated and described in previous studies [2,3]. For the positron annihilation experiments, 1-mm thick pieces of 10×10 mm^2 size were used. Pairs of samples were solutionised at 540 °C for 1 h in an Ar atmosphere. Mainly two quenching procedures were applied. (i) Water quenching (QW): the samples fall through a vertical glass tube from the heating zone into ice water. While falling, the samples are kept inside a metal heat shield and reservoir out of which they are ejected just above the water level, thus avoiding premature cooling. (ii) Solid state quenching (QS): the samples are manually removed from a furnace and rapidly put onto a copper block precooled with liquid nitrogen. Then, a second precooled copper block is placed on top of the samples within less than 0.5 s, thus leading to very good thermal contact. QW provides only slightly higher quenching rates as seen from the initial positron lifetime value (see results and discussion part), but QS allows us to process the quenched samples at low temperatures, thus preventing ageing during mounting. After quenching, the samples were dried (only for QW) and mounted to a sandwich containing the positron emitter (^{22}NaCO$_3$ in a Kapton® envelope) in between. For QS mounting was carried out in a glove box at a sufficient low temperature to avoid the condensation of humidity on the sample, for QW mounting was done at 'room temperature'.

2.2 Positron annihilation lifetime spectroscopy and data analysis

Two spectrometers were used. The one at the laboratory in Berlin (**B**) is an analog fast-fast coincidence spectrometer with photomultiplier tubes H3378-50 from Hamamatsu and BaF$_2$ scintillators. Backscattering was supressed by lead shields [21]. The count rate achieved was usually 700-800 s^{-1}. Spectra typically contained ~10^5 counts for spectra measured in-situ in about 2 min, and ~2×10^6 counts in spectra meant for lifetime component decompositions. The measured positron lifetime spectra contain contributions from the 20 μCi ^{22}Na$_2$CO$_3$ source itself. We used spectra measured on pure annealed Al and Si to determine the contributions of the positron source to the measured spectra. They contain a component of about 11% from the two 7.5-μm thick Kapton foils and the sodium salt (both ~0.400 ns) and less than 1% of a component with a long lifetime due to positronium formation at surfaces and pores (~3 ns). Determination of the source corrections of Kapton and salt was carried out for each of the different measurement temperatures independently to account for a possible temperature dependence, which, however, was found to be negligible in accordance to Ref. [22]. For the positronium component, we adopted the strategy outlined in Ref. [3] to treat the lifetime and intensity of that component as a variable at low temperatures and to check whether it takes reasonable values after fitting. The program LT9 was used to subtract the source contributions as well as the background and to de-convolute the spectra from the spectrometer resolution function which we found to be well represented by one Gaussian with a FWHM of ~0.220 ns. The spectrometer is attached to a liquid nitrogen cooled cryostat which allows for measurements at any temperature down to −180 °C.

The spectrometer in Prague (**P**) [23] is digital and optimised for high resolution (FWHM of resolution function is 0.145 ns) but has a lower count rate of 50 s^{-1}. The spectrometer is equipped with BaF$_2$ scintillators optically coupled to Hamamatsu H3378-50 photomultiplier tubes. Pulses from the detectors are sampled by a pair of Acqiris DC211 digitisers at a rate of 4 GHz. A 27 μCi ^{22}Na$_2$CO$_3$ positron source is sealed by a 2-μm thick titanium foil. Decomposition of positron lifetime spectra is analogous to the treatment in Berlin except that the spectrometer resolution function is modelled by two Gaussians [24]. The source contribution to the positron lifetime spectra was determined using a reference sample of well annealed Al and contained of two components with lifetimes 0.180 ns and 0.400 ns and relative intensities 10% and 2%, respectively. These components represent a contribution of positrons annihilated in the Ti foil and the Na$_2$CO$_3$ positron source spot, respectively. 5×10^6 counts were obtained for each spectrum which took typically 1 day. All the measurements were carried out at −150 °C.

One-component positron lifetimes τ_{1C} are obtained by fitting one decaying exponential represented by one lifetime component to a measured data set. If the spectrum contains more than one component the fit might not be satisfactory, reflected by oscillations in the fitting residual and a higher than usual fit variance. The closer the two components lie together the more likely they appear as one component. The resulting lifetime will not necessarily be the weighted average of the two components since the fitting program might change other parameters such as the spectrometer resolution or the positronium component to obtain optimal fits.

If there is evidence for 2 or even 3 components one can try a multi-component fit. The residual and variance should improve notably to justify such an approach. The high-resolution spectrometer **P** allowed us to fit three lifetime components and to obtain 5 free parameters (3 lifetimes, 2 intensities). The lower resolution of spectrometer **B** allows us to determine only two lifetime components. Fits with 2 free positron lifetime and one intensity are feasible for diluted binary Al-Mg and Al-Si alloys [25], however, such fits become instable for the alloy considered here because the two components lie closer together. Therefore, we fixed the vacancy-related lifetime component to 0.245 ns and varied just the second lifetime and its intensity. This we shall call '1½-component' fit in this paper.

Measured positron lifetimes shall be displayed as quantities indexed with numerals, τ_1, τ_2, τ_3, whereas positron lifetimes at defined locations are indexed with letters for **b**ulk, **s**olute clusters (shallow positron traps), **v**acancy-related defects (deep positron traps), $\tau_\mathrm{b}, \tau_\mathrm{s}, \tau_\mathrm{v}$, following the usual convention [20]. According to the three-state trapping model (3STM) [20] each of the measured lifetimes (1,2,3) corresponds to one of the annihilating objects (b,s,v) and we maintain this order in the following.

3. Results

Fig. 1a contains various sets of measurements of the one-component positron lifetime during NA of the alloy (some of the data has been presented before [26], but has been analysed differently, namely with a fixed positronium lifetime and a free intensity). The first run (green open circles) was measured at 20 °C and shows the four stages described in the introduction and reported in Ref. [3]. The absolute values are about 0.01 ns higher than in Ref. [3], but the overall course is nearly identical. Such slight

offsets between different spectrometers are normal for this type of measurement [21].

In a second run, the sample was put into a cryostat directly after water quenching (QW). Exposure to 'room temperature' was about 5 min in this case. Measurements at four decreasing temperatures (−60 °C, −100 °C, −140 °C, −180 °C, blue full triangles) point at a pronounced temperature dependence. After reheating to 20 °C (in about 1-2 min), ageing continued (red open diamonds). The sample was cooled again after in total 30 min of NA and re-measured at the same four temperatures. The same was done again after ageing for in total 80, 140 and 900 min. A third run (blue open triangles) was based on solid state quenching (QS) which avoids even short exposure to 'room temperature' after quenching. The corresponding data is included in Fig. 1a. The data acquired at low temperature contained enough statistics to be treated by '1½-component fitting', whereas this was not possible for the spectra measured in-situ at 20 °C, where only a one-component positron lifetime could be obtained.

Fig. 1b displays the temperature dependence of the measurements as relative changes with respect to the reference temperature −60 °C, i.e. $\Delta\tau_{1C} = \tau_{1C}(T) - \tau_{1C}(-60\,°C)$. The temperature dependence is strongest after 5 min of NA and levels off after without disappearing even after 900 min of NA. Even the as-quenched ('AQ') sample exhibits a pronounced dependence of τ_{1C} on temperature.

Fig. 2a shows decompositions of the measured positron lifetime spectra into various components. Data measured with the high-resolution spectrometer **P** at −150 °C were used to obtain three lifetime components (τ_1, τ_2, τ_3) and the corresponding intensities (I_1, I_2, I_3). These are displayed as $\tau_i(I_i)$ plots where NA time is an implicit parameter (see labels). Measurements were carried out for 5 min (NA during assembly of

sample), 30, 50, 70, 140, 1000, 4000 and 10000 min. NA for 140 min and longer yielded just one component. After NA for 30, 50 and 70 min, three components were identified, after NA for 5 min just two. The vacancy-related component τ_3 dominates after 5 min of ageing (85% intensity) but is reduced to 50% after 70 min of NA, shortly before stage II has ended. Correspondingly, the other components increase. There is a component τ_2 ranging from 0.210 to 0.220 ns throughout stage II, which is thought to reflect positron annihilation in solute clusters and increases from initially 25% to 45% during stage II, after which it goes up to 100%. Moreover, a small reduced bulk component τ_1 around 0.025 ns can be detected in some samples.

Data measured with spectrometer **B** just allowed for 1½-component fits with the vacancy-related lifetime fixed to 0.245 ns. The results of the three-component fits with spectrometer **P** actually justify this choice since τ_3 remains close to 0.245 ns throughout ageing. For the measurements carried out at −140 °C, Fig. 2a shows the second component that represents the combined bulk and solute cluster components in the three-component fit and is therefore labelled 'τ_{1+2}'. In order to compare the measurements carried out with spectrometers **P** and **B**, the three-component data from spectrometer **P** is converted to a virtual two-component fit by adding up the two shorter lifetimes using:

$$\tau_{1+2} = \frac{I_1}{I_{1+2}}\tau_1 + \frac{I_2}{I_{1+2}}\tau_2, \ \text{with} \ I_{1+2} = I_1 + I_2. \tag{1}$$

This data (open diamonds) are qualitatively the same as the data from the 1½-component fit (full diamonds) for the longer NA times. For short NA there are deviations but the trend is the same: the combined component τ_{1+2} grows at the cost

of the vacancy-related component during NA and crosses the value for pure defect-free aluminium (0.160 ns).

Fig. 2b shows data for τ_{1+2} and τ_3 obtained in-situ during ageing of quenched samples (QS) at three temperatures at or below 0 °C (spectrometer **B** was used). Data obtained at room temperature cannot be decomposed into two components in a reliable way due to the too fast ageing and the corresponding low number of counts in each spectrum. The curves for the different temperatures are similar. Moreover, the similarities between Fig. 2a and b are evident, namely the increase from positron lifetimes τ_{1+2} well below the lifetime in pure Al (0.160 ns) and corresponding low intensities for short ageing times to a positron lifetime well above this value (around 0.220 ns) with ~85% intensity, i.e. predominant trapping into one kind of trap (the intensity does not go to 100% contrary to the impression created in Fig. 2b, which is caused by the large statistical scatter of the data).

Fig. 3 shows the course of the one-component lifetime during NA of samples quenched into different quenching media: water at 0 °C (QW) and 20 °C, ethanol at 0°C, liquid nitrogen and a copper block cooled by liquid nitrogen (QS). We notice a different starting value of the lifetime after quenching, a merger of all lines after ~80 min (end of stage II) and the same development up to 1000 min (around the end of stage III).

4. Discussion

4.1 General course of lifetime development

The one-component positron lifetimes measured in-situ at 20 °C exhibits the stages labelled in Fig. 1a and confirm earlier measurements. Stage I is too short at 20 °C

ageing temperature to be detected. It appears clearly at lower temperatures or higher contents of Mg and Si and also depends on the quenching conditions [17]. In this work, the main interest is in stages II and III which will be discussed in the following. Stage IV is a final coarsening or ordering effect not relevant in the context of this work.

The temperature dependence found confirms previous experiments. For a similar alloy, Klobes [19] found a higher $\Delta\tau$ = 0.008 ns for 30 min of NA in the same temperature interval (he did not investigate as-quenched samples) and also reported that $\Delta\tau$ went to 0 faster with progressing NA than in this study.

The course of the combined lifetime τ_{1+2} in Fig. 2a and b directly shows that a new kind of positron trap not related to vacancies is formed during NA. The possibility mentioned in the introduction, namely that the excess vacancies present after quenching are eliminated during NA and positrons increasingly annihilate in the bulk can be ruled out. Although under such circumstances one would measure a decrease of the measured one-component lifetime from 0.250 ns (free vacancy) towards the value for the aluminium bulk (0.160 ns), the partial component τ_{1+2} would behave differently as one can see from the simple trapping model (which is the limiting case of the three-state trapping model introduced in the next section) [20]. Accordingly, in such a case, two lifetimes and intensities can be measured, τ_1, τ_2, I_1, I_2, which are related by:

$$\tau_1 = I_1 \left(\frac{1}{\tau_b} - \frac{I_2}{\tau_2} \right)^{-1},\qquad(2)$$

with τ_b = 0.160 ns being the lifetime of positrons in bulk defect-free aluminium. Obviously, $\tau_1 < \tau_b$ in this case for any $I_1 \in [0,1]$ and $\tau_2 > \tau_b$. We would therefore

obtain a curve for τ_1 approaching the value for 0.160 ns from below without crossing the broken horizontal lines in Fig. 2, which is not what the measurement shows. The measured curve is therefore initially dominated by positron annihilation in vacancies or vacancies attached to atoms. In the course of ageing, annihilation is increasingly in the new positron trap (thought to be related to vacancy-free solute clusters) with a lifetime around 0.210 to 0.220 ns. The combined lifetimes in the bulk and such traps can therefore be anywhere below 0.210 ns and cross the line at τ_b = 0.160 ns.

4.2   Modelling of positron lifetime as a function of temperature

For a quantitative discussion of the temperature-dependent lifetimes in Fig. 1 we will now use the three-state trapping model (3STM) for positron trapping and annihilation involving two kinds of positron traps and the bulk of the material. Vacancy-related defects provide a deep potential well of ~2 eV depth for positrons [27], which means that they cannot escape after being trapped since their mean thermal energy is just 40 meV at 20 °C. Vacancy-free solute clusters, in contrast, are shallower potentials with depths depending on the cluster composition [20,28]. In some cases, the potential well represented by vacancy-free solute clusters becomes comparable to the thermal energies of a positron. Such (coherent) clusters can trap positrons provided their size is above a certain limit which depends on the positron affinity of the solute elements involved. These are A = −6.18 eV for Mg, A = −6.95 eV for Si and A = −4.41 eV for Al [29]. The critical value for trapping, for example in pure Si clusters in Al, is given by: $r_{Si} = \frac{0.58\,\text{nm}}{\sqrt{A_{Al} - A_{Si}}}$, with A in [eV] [30]. With this, r_{Si} = 0.36 nm, and similar for Mg or mixed Mg-Si clusters. Therefore, already a few atoms in a cluster can actually trap positrons and give rise to a detectable signal.

If the depth of a potential well associated to a solute cluster is low, a positron can be de-trapped at a considerable rate from such a cluster, which favours competing trapping into deep traps if there are such. The de-trapping rate depends on the temperature: the lower the thermal energy of the positron, the more difficult de-trapping becomes or, in other words, at low temperatures shallow traps become deep traps. If deep and shallow traps co-exist, the measured positron lifetime will depend on temperature if positrons have a different lifetime in the two since their relative contribution to annihilation varies with temperature. To deal with the temperature dependence in our experiments we now assume that one of the traps is shallow and one is deep due to the presence of solute clusters (s) and vacancy-related defects (v), respectively. The processes involved are depicted in Fig. 4: positrons are injected into the bulk of the alloy and thermalize there after a few ps. They are trapped by the two kinds of traps, each at a rate κ_i. From the shallow trap 's' they get back into the bulk at a rate δ_s while they remain in the deep trap 'v'. Eventually, the positrons are removed from the system by annihilation at a rate λ_i characteristic for the three possible annihilation sites. All these transitions are governed by rate equations that can be solved and yield expressions for the measurable lifetime components and corresponding intensities [20]. These equations are the starting point for our analysis:

$$\tau_1 = \frac{2}{\lambda_b + \kappa_s + \kappa_v + \lambda_s + \delta_s + \sqrt{(\lambda_b + \kappa_s + \kappa_v - \lambda_s - \delta_s)^2 + 4\delta_s \kappa_s}}, \tag{3}$$

$$\tau_2 = \frac{2}{\lambda_b + \kappa_s + \kappa_v + \lambda_s + \delta_s - \sqrt{(\lambda_b + \kappa_s + \kappa_v - \lambda_s - \delta_s)^2 + 4\delta_s \kappa_s}}, \tag{4}$$

$$\tau_3 = \lambda_v^{-1}, \tag{5}$$

$$I_1 = 1 - I_2 - I_3, \tag{6}$$

$$I_2 = \frac{\delta_s + \lambda_s - \tau_2^{-1}}{\sqrt{(\lambda_b + \kappa_s + \kappa_v - \lambda_s - \delta_s)^2 + 4\delta_s\kappa_s}} \left(1 + \frac{\kappa_s}{\delta_s + \lambda_s - \tau_2^{-1}} + \frac{\kappa_v}{\lambda_v - \tau_2^{-1}}\right), \tag{7}$$

$$I_3 = \frac{\kappa_v(\delta_s + \lambda_s - \lambda_v)}{(\lambda_v - \tau_1^{-1})(\lambda_v - \tau_2^{-1})}. \tag{8}$$

It is now necessary to find values for the six rates $\lambda_b, \lambda_v, \lambda_s, \kappa_s, \kappa_v, \delta_s$ in Fig. 4 and on the r.h.s. of Eqs. (3-8) that yield the six measured quantities on the l.h.s. λ_b expresses the positron annihilation rate in defect-free Al (0.160 ns) and is set to $\lambda_b = \frac{1}{0.160}$ ns^{-1}. λ_v is the positron annihilation rate in defects in the aluminium matrix related to a vacancy. This annihilation rate is $\lambda_v \sim \frac{1}{0.250}$ ns^{-1} for a single vacancy in an Al matrix. If a vacancy is associated to one or more Si or Mg atoms the annihilation rate is expected to be higher or (only slightly) lower, respectively, than this value but the changes are expected to be small [21]. We therefore approximate the distribution of different annihilation rates by a mean value of $\lambda_v = \frac{1}{0.245}$ ns^{-1}. The inverse of the mean value of the annihilation rate agrees well with the values for τ_3 in Fig. 2a, using Eq. (5). The positron lifetime in vacancy-free clusters of Mg, Si and Al atoms has been postulated to be typically around 0.200 ns [21] or up to 0.215 ns [16]. We found that the stage II of decreasing lifetime can be modelled very well by choosing the corresponding annihilation rate $\lambda_s = \frac{1}{0.210}$ ns^{-1}.

The trapping (κ_s, κ_v) and detrapping (δ_s) rates have to be determined by fitting the 3STM to experimental data. δ_s will be temperature-dependent since positrons with a higher energy at higher temperatures will more easily escape from the shallow traps than low-energy positrons. We use an expression for δ_s applicable to small clusters [31,32]:

$$\delta_{\mathrm{s}} = \frac{\kappa_{\mathrm{s}}}{c_{\mathrm{s}}} \left(\frac{m^* k_{\mathrm{B}} T}{2 \pi \hbar^2} \right)^{1.5} e^{-\frac{E_{\mathrm{s}}}{k_{\mathrm{B}} T}}, \tag{9}$$

where c_{s} is the number density of shallow traps, m^* the effective mass of the positron and E_{s} the binding energy between positron and shallow traps. We approximate m^* by the electron mass m_{e} and are left with two more unknown parameters, c_{s} and E_{s}.

We use the data set for the sample NA for 5 min to determine the 4 parameters $\kappa_{\mathrm{s}}, \kappa_{\mathrm{v}}, c_{\mathrm{s}}$ and E_{s}. Spectra were measured for 4 temperatures, see blue full triangles in Fig. 1a, and decomposed into two lifetime components, (τ_{1+2}, I_{1+2}) and (τ_3, I_3) (components for −140 °C given in Fig. 2a, others are available). Eqs. (3-8) were used in conjunction with Eq. (1) to fit the experimental $\tau_{1+2}(T)$ and $I_{1+2}(T)$ as well as the total average lifetime:

$$\tau_{\mathrm{av}} = \sum I_i \tau_i. \tag{10}$$

Fig. 5a and b demonstrate that the measured lifetimes τ_{av}, τ_{1+2} and intensities I_{1+2} can be represented well by the equations of the 3STM. Fig. 5b shows that a temperature increase leaves the small reduced bulk component (I_1, close to the detection limit) almost unchanged but increases annihilation in the vacancy-related defects (I_3) at the cost of annihilation in the shallow traps (I_2). This is because the de-trapping rate δ_{s} increases with temperature. For $T \to 0$ the lifetimes level off since the de-trapping rate approaches 0 and the temperature dependence is then marginal. Values of κ_{s} = 33 ns^{-1} and κ_v = 29 ns^{-1} were determined by fitting. At this stage of ageing, trapping into the two kinds of traps is therefore comparable. The other parameters found were the binding energy of positrons with the shallow traps E_{s} = 16.4 meV and the number density of shallow traps c_{s} = 2.4×10^{25} m^{-3}. Klobes [19] found

a very similar value of E_s = 21 meV, however treating the detrapping process differently. The value for c_s can be compared to the number density of all the solute atoms in the alloy which is 4.8×10^{26} m^{-3}, i.e. 20 times higher. If all the solute had partitioned into clusters after 5 min of NA, each cluster would therefore contain 20 solute atoms on average. However, it is much more likely that most of the solute is still distributed in the supersaturated solid solution at this stage and the clusters contain much fewer solute atoms. A density of vacancy-related defects c_v can be calculated using the relation $\kappa_v = \mu\, c_v$ and the positron trapping coefficient μ for one vacancy [33,34], namely $\mu = 2.5 \times 10^{14}$ s^{-1}. The resulting data are compiled in Table 1. Accordingly, the vacancy density is only slightly below the equilibrium density at 540 °C, while the cluster density is three times higher. This indicates that most vacancies are preserved during quenching and short subsequent NA. Simulations of vacancy annihilation at grain boundaries and dislocation jogs during quenching have shown that a quenching rates of 1000 Ks^{-1} is sufficient to largely supress vacancy losses [35] in accordance with the experimental finding. Solute cluster densities are so high because positrons can be trapped even in very small clusters, which can be very numerous at this stage. Kinetic Monte Carlo simulations based on parameters generated by ab-initio calculations have yielded solute cluster densities that can easily reach or even exceed the values measured here after a few minutes of NA, but these densities include a large number of dimers and trimers that might not contribute to positron annihilation [36]. Atom probe measurements on the other hand, have mostly been carried out on alloys richer in Si and Mg and for much longer NA times. Some number densities measured were 3×10^{24} m^{-3} after 7 d of NA [9], 2×10^{23} m^{-3} after 3.5 h of NA [37] and 6.8×10^{23} m^{-3} after 2 weeks of NA [38], all in alloys higher in Mg and Si. 2

months of NA [15] in an alloy similar to the one investigated here yielded a solute cluster density 4.3×10^{23} m^{-3}. Therefore, by positron annihilation we obtain higher values after 5 min of NA, but atom probe data might not include very small clusters and also there might have been considerable coarsening after the long NA times that are usually included in such studies. A direct verification of our results is therefore not possible but calculations and experiments indicate that positron annihilation yields the correct order of magnitude for the solute cluster density.

4.3   Representation of positron lifetime as a function of NA time

We now represent the time evolution of the positron lifetime and its temperature dependence. The fitting procedure in the previous section provides values for the various (de)trapping rates involved after 5 min of ageing. The task is now to set up a scenario how these parameters vary during NA. Unfortunately, a representation of the measured temperature-dependent positron lifetimes for other than 5 min of NA did not yield stable enough fits to yield usable rates. We shall therefore go the reverse way: to assume a plausible representation of the time dependence of the rates, to apply the three-state trapping model and to compare the calculated evolution of the temperature dependent positron lifetime with NA time. Due to the large number of adjustable parameters this approach cannot be as strict as the one in the previous section and merely serves as a visualisation of the measured data.

In order to simplify the scenario we first assume that the binding energy E_s and the ratio $\frac{\kappa_s}{c_s}$ in Eq. (9) remain constant throughout NA. With increasing numbers of aggregated atoms the potential well associated with clusters will grow in spatial extension, but its depth will remain similar and hereby E_s. κ_s and c_s will change but

their ratio represents a trapping rate per positron trap, the change of which will be less pronounced upon cluster growth (this approximation will be discussed later in this section). In contrast to these parameters, κ_s and κ_v will approximately scale with the density of the two types of traps and vary a lot. κ_v scales with the vacancy density in the alloy which is $c_v \sim 1.4 \times 10^{-4}$ during solutionising and after quenching as can be calculated by using the formation energy of a vacancy and the quenching temperature in an Arrhenius equation [36]. During ageing, the vacancies assist in transporting solutes to clusters. As the total solute concentration is 8×10^{-3} in our alloy – containing $\sim$0.4% of both Mg and Si – each vacancy has to transport $\sim$60 solute atoms if all solutes are eventually delivered. Therefore, vacancies must be preserved for a long time and exist either attached to solute atoms or inside clusters throughout ageing and their density will never go to zero. This indirect argument is experimentally supported by studies on binary Al-Mg alloys where it was found that other than in Al-Si alloys, vacancies cluster together during NA at a much lower rate and are separate entities throughout ageing, probably attached to Mg atoms [25]. Mg therefore stabilises individual vacancies in Al-Mg and it seems likely that it also does this in Al-Mg-Si alloys. TEM investigations have also led to this conclusion [39]. However, we account for some losses of vacancies to grain boundaries, dislocation loops etc., by assuming that the vacancy density decays exponentially to a non-zero saturation value. For the density of solute clusters (shallow traps) we assume that it increases exponentially from zero directly after quenching (which we later will find is not realistic) to a finite value. For the annihilation rates λ_b and λ_v we state that they remain constant. λ_s however, cannot be constant since the positron lifetime increase after 80 min of NA visible in Fig. 1a would not be explainable in this case. It has been argued that the

diffusion of Mg into the emerging clusters causes an increase of the lifetime of positrons annihilating within and it appears reasonable to assume that the associated rate λ_s decreases during NA. For the variable parameters we therefore write:

$$\kappa_v = \kappa_v^0 - \Delta\kappa_v\left(1 - e^{-t/t_v}\right), \ \kappa_s = \Delta\kappa_s\left(1 - e^{-t/t_s}\right)$$

and $\lambda_s^{-1} = 0.210 \text{ ns} + \Delta\lambda_s\left(1 - e^{-t/t_\lambda}\right).$ \hfill (11)

Here, t_v, t_s and t_λ are three time constants and κ_v^0, $\Delta\kappa_v$, $\Delta\kappa_s$ and $\Delta\lambda_s$ are adjustment parameters that ensure that the parameters vary within the desired range. The exponential laws express that the changes are strongest directly after quenching and gradually fade out. They have been applied by other authors too [40]. We use the values obtained by fitting the data for 5 min of NA as a boundary condition in Eq. (11) but due to the large number (seven) of free parameters in Eq. (11) it is impossible to fit the experimental results to the model directly. Rather we set the parameters in a manual selection process aiming at reproducing the course of the data in Fig. 1a and b qualitatively.

The resulting lifetimes are shown in Fig. 6. Comparing with Fig. 1, we note the similarity of the general course of positron lifetime and especially of the temperature dependence in Fig. 1b. The numerical values cannot be expected to coincide in view of the simplicity of the model. Moreover, one-component lifetimes τ_{1C} tend to slightly differ from averaged lifetimes τ_{av} calculated from the individual components due to the difficulty of reliably detecting all the components of positron spectra. Especially the short reduced bulk component τ_1 cannot be measured precisely.

If λ_s is assumed to be constant, i.e. $\Delta\lambda_s = 0$ in Eq. (11), the calculated positron lifetime monotonically decreases during ageing and there is no stage III of increasing lifetime. However, if we allow λ_s to decrease, the experimentally known increase of positron lifetime in stage III is nicely reproduced.

The variations of positron lifetime shown in Fig. 1b and Fig. 6b look very similar except that the absolute scale differs again. In the as-quenched state, the model predicts no temperature dependence since only vacancy-related defects are present. Therefore, the experiment clearly demonstrates that even without any NA, solute clusters must have already formed in the alloy during quenching and act as shallow traps since the sample labelled 'AQ' in Fig. 1a was quenched to very low temperatures directly and measured without any exposure to 'room temperature' (always keeping it at $T <$ −100 °C). The measured 'AQ' value in Fig. 6b therefore rather corresponds to a short ageing time in reality (see arrow). The influence of shallow traps peaks after 5 min of NA, after which it decreases again. The fact that there is a minimum of $\Delta\tau$ for intermediate NA time can be easily explained. For $t = 0$ all traps (vacancy-related) are deep (at least theoretically), and there is no temperature dependence of τ_{av}. For $t =$ 100 min, the concentration of solute clusters is much higher than that of the vacancy-related traps and therefore the temperature dependence also gets small since almost all positrons annihilate in the clusters at all temperatures. It is the competition between deep and shallow traps that gives rise to the temperature dependence in Fig. 6b and this is highest for short ageing times.

Fig. 6c specifies some of the parameters used in the model. We see how trapping into vacancies decreases in the course of NA while trapping in clusters increases.

Eventually, after 2000 min of NA, κ_s reaches ~6 times the value determined for 5 min of NA. We treated $\frac{\kappa_s}{c_s}$ in Eq. (9) as a constant in our model. The higher κ_s would then imply an equally high c_s, but in reality it could also be caused by a larger trapping coefficient μ, e.g. because the solute clusters have grown or changed their composition. Therefore the course of c_s during NA cannot be predicted without more knowledge of the positron trapping properties of solute clusters. c_s could also level off during NA and solute clusters could even coarsen, leading to a decreasing c_s. Other factors might play a role and modify the scenario: E_s could be varying during ageing, for example, the cluster potential could become deeper and correspondingly E_s higher as the clusters grow and/or change their composition. This has been claimed based on calculations [41]. Such an increase would reduce the temperature dependence for longer NA times. Moreover, it is realistic to assume that solute clusters of different sizes co-exist and that their distribution evolves with time. Also, the size and configuration of vacancy-related defects can be expected to change during ageing. Therefore, we expect a time-dependent distribution of positron lifetimes instead of two fixed sharp values, but this cannot be measured.

In conclusion, however, it is apparent that the main features of positron lifetime evolution during NA can be captured by the three-state trapping model and the simple assumptions leading to the representations in Fig. 6 appear reasonable although the rates determined and given in Fig. 6a should not be taken too literally.

4.4   Quenching experiments

Fig. 1 indicates that even after quenching at a high rate, solute clusters are present in the sample and trap positrons. In order to support this conclusion independently we

carried out various experiments in which samples were quenched into media at different temperatures and of different composition. Although we cannot measure quenching rates directly, we know that the rate will be lower if the medium water has a higher temperature [42]. Moreover, ethanol with its higher vapour pressure will exhibit even lower quenching rates due to increased gas film formation during quenching. Quenching into liquid nitrogen is known to lead to low quenching rates due to an extensive Leidenfrost phenomenon. Solid state quenching between two cold copper blocks (QS) is another option.

Obviously, the starting value of positron lifetime obtained after quenching differs between the various experiments as shown in Fig. 3. Water quenching at 0 °C (QW) yields the highest value, solid state quenching (QS) the second. The suspected lower quenching rates of the other quenching experiments lead to further reductions. It is near at hand to explain this by an increased solute cluster formation during quenching in the experiments carried out with a lower quenching rate. More time is spent at high temperatures where atomic mobility is increased and diffusion is fast. The associated higher fraction of positron trapped in solute clusters will then decrease the average values measured since positrons live shorter in solute clusters than in vacancy-related defects. Hence, positron annihilation can detect changes of the quenching rate with great sensitivity. After ~80 min (end of stage II), all samples reach the same value of one-component lifetime, indicating that all possible solute clusters have formed regardless how fast quenching has been. The further course of lifetime evolution which is dominated by the increasing Mg-content of solute clusters is the same in all the experiments.

5. Conclusions

We investigate an Al-Mg-Si alloy containing 0.4 wt.% Mg and 0.4 wt.% Si during natural ageing by applying positron annihilation lifetime spectroscopy and find:

- Directly after quenching, even if care is taken to avoid any exposure to 'room temperature' natural ageing, two types of positron traps can be detected in the sample: vacancy-related defects (i.e. free vacancies or vacancies associated to solute atoms or clusters) and vacancy-free solute clusters. The former account for more than 80% of the positron annihilation signal.

- Slower quenching rates give rise to a larger extent of cluster formation.

- During natural ageing up to 80 min, the vacancy contribution to the positron annihilation signal continuously drops while the solute cluster signal increases up to 70%, indicating an increasing number of solute clusters that compete with the vacancy-related defects. This change of contributions brings the measured positron lifetime down to a minimum after 80 min (during stage II, using the notation of a previous publication).

- The ageing process continues after stage III has started (increasing positron lifetime). After 140 min of NA (or earlier) the solute clusters dominate and the positron annihilation signal from the vacancy-related defects can no longer be separated, which means that their contribution has dropped to below ~10%. However, they must be present since the positron lifetime is still temperature-dependent and also because without vacancies diffusional processes would terminate. Positron lifetime increases due to the lower annihilation rate in the solute clusters, most likely caused by the increased content of Mg atoms.

The scenario consistent with these measurements is: quenching from 540 °C preserves a high density of excess vacancies at low ('room') temperatures, but already during quenching solute clustering sets in. The vacancies bind to solute-vacancy complexes and transport solute atoms to emerging clusters. The vacancies spend time at or in the solute clusters and eventually detach to diffuse to new solute atoms. During subsequent natural ageing, more and more solute clusters form and grow. As the number of vacancies is so low (~2 orders of magnitude lower than the number of solute atoms) most clusters are vacancy-free and coherent to the surrounding matrix. Only a minority of the solute clusters contains vacancies at a given time, but a vacancy-free solute cluster can temporarily turn into a vacancy-containing one, after which it converts back into a vacancy-free cluster.

Modelling of the positron lifetime data with the three-state trapping model provides a description of all features measured and estimates for cluster and vacancy densities.

Acknowledgements

References

[1]   C. Panseri, T. Federighi, J. I. Met. 94 (1966) 99-197.

[2]   J. Banhart, C.S.T. Chang, Z.Q. Liang, N. Wanderka, M.D.H. Lay, A.J. Hill, Adv. Eng. Mater. 12 (2010) 559-571.

[3]   J. Banhart, M.D.H. Lay, C.S.T. Chang, A.J. Hill, Phys. Rev. B 83 (2011) 014101.

[4]   C.S.T. Chang, I. Wieler, N. Wanderka, J. Banhart, Ultramicroscopy 109 (2009) 585-592.

[5]   M.L.V. Gayler, G.D. Preston, J. I. Met. 41 (1929) 191-247.

[6]   L.F. Cao, P.A. Rometsch, M.C. Couper, Mat. Sci. Eng. A 559 (2013) 257-261.

[7]   M. Murayama, K. Hono, M. Saga, M. Kikuchi, Mat. Sci. Eng. A 250 (1998) 127-132.

[8]   M. Murayama, K. Hono, Acta Mater. 47 (1999) 1537-1548.

[9]   A.I. Morley, M.W. Zandbergen, A. Cerezo, G.D.W. Smith, Mater. Sci. Forum. 519-521 (2006) 543-548.

[10]   D. Vaumousse, A. Cerezo, P.J. Warren, S.A. Court, Mater. Sci. Forum. 396-4 (2002) 693-698.

[11]   F. De Geuser, W. Lefebvre, D. Blavette, Phil. Mag. Lett. 86 (2006) 227-234.

[12]   A. Serizawa, T. Sato, 3DAP characterisation of two types of nanoclusters and bake-hardening behavious of Al-Mg-Si alloys, in: B.S. J. Hirsch, G. Gottstein (Eds.), Proceedings of the 11th International Conference on Aluminium Alloys (ICAA11), Aachen, 2008, pp. 915-921.

[13]   A. Serizawa, S. Hirosawa, T. Sato, Metall. Mater. Trans. A 39A (2008) 245-251.

[14]   A. Serizawa, T. Sato, W.J. Poole, Phil. Mag. Lett. 90 (2010) 279-287.

[15]   M. Torsaeter, W. Lefebvre, S.J. Andersen, C.D. Marioara, J. Walmsley, R. Holmestad, Clustering behaviour in Al-Mg-Si alloys investigated by APT, in: S.

Kumai, O. Umezawa, Y. Takayama, T. Tsuchida, T. Sato (Eds.), Proceedings of the 12th International Conference on Aluminium Alloys (ICAA12), Yokohama, 2010, pp. 1385-1390.

[16]   M.D.H. Lay, H.S. Zurob, C.R. Hutchinson, T.J. Bastow, A.J. Hill, Metall. Mater. Trans. A 43A (2012) 4507-4513.

[17]   M. Liu, Clustering kinetics in Al-Mg-Si alloys investigated by positron annihilation techniques, (Ph.D. thesis), Technische Universität Berlin, 2014.

[18]   B. Klobes, T.E.M. Staab, M. Haaks, K. Maier, I. Wieler, Phys. Stat. Sol. 2 (2008) 224-226.

[19]   B. Klobes, Strukturelle Umordnungen in Aluminiumlegierungen:ein komplementärer Ansatz aus der Perspektive von Leerstellen und Fremdatomen, (Ph.D. thesis), University of Bonn, 2011.

[20]   R. Krause-Rehberg, H.S. Leipner, Positron Annihilation in Semiconductors, Springer, Heidelberg, 1999.

[21]   J. Banhart, M. Liu, Y. Yan, Z.Q. Liang, C.S.T. Chang, M. Elsayed, M.D.H. Lay, Physica. B 407 (2012) 2689-2696.

[22]   M.A. Monge, J.d. Rio, J. Phys.: Condens. Mat. 6 (1994) 2643-2646.

[23]   F. Bečvář, J. Čížek, I. Procházka, J. Janotová, Nucl. Instrum. Meth. A 539 (2005) 372-385.

[24]   I. Procházka, I. Novotný, F. Bečvář, Mater. Sci. Forum. 255-257 (1997) 772-774.

[25]   M. Liu, Y. Yan, Z.Q. Liang, C.S.T. Chang, J. Banhart, Influence of Mg and Si atoms on the cluster formation process in Al-Mg-Si alloys studied by positron annihilation lifetime spectroscopy, in: H. Weiland, A.D. Rollett, W.A. Cassada

(Eds.), Proceedings of the 13th International Conference on Aluminium Alloys (ICAA13), Pittsburgh, 2012, pp. 1131-1137.

[26] M. Liu, J. Čížek, C.S.T. Chang, J. Banhart, Mater. Sci. Forum. 794-796 (2014) 33-38.

[27] M. Puska, R.M. Nieminen, J. Phys. F 13 (1983) 333-346.

[28] G. Dlubek, Mater. Sci. Forum. 13-14 (1987) 11-32.

[29] M.J. Puska, P. Lanki, R.M. Nieminen, J. Phys.: Condens. Mat. 1 (1989) 6081-6093.

[30] M.J. Puska, J. Phys.: Condens. Mat. 1 (1989) 7347-7366.

[31] M. Manninen, R.M. Nieminen, Appl. Phys. A 26 (1981) 93-100.

[32] K. Saarinen, P. Hautojarvi, A. Vehanen, R. Krause, G. Dlubek, Phys. Rev. B 39 (1989) 5287-5296.

[33] E. Gramsch, K.G. Lynn, Phys. Rev. B 40 (1989) 2537.

[34] J.A. Jackman, G.M. Hood, R.J. Schultz, J. Phys. F 17 (1987) 1817-1831.

[35] F.D. Fischer, J. Svoboda, F. Appel, E. Kozeschnik, Acta Mater. 59 (2011) 3463-3472.

[36] Z.Q. Liang, C.S.T. Chang, C. Abromeit, J. Banhart, J. Hirsch, Int. J. Mater. Res. 103 (2012) 980-986.

[37] P.A. Rometsch, L.F. Cao, X.Y. Xiong, B.C. Muddle, Ultramicroscopy 111 (2011) 690-694.

[38] S. Pogatscher, H. Antrekowitsch, H. Leitner, T. Ebner, P.J. Uggowitzer, Acta Mater. 59 (2011) 3352-3363.

[39] G. Thomas, J. I. Met. 90 (1961) 57-63.

[40] A. Somoza, A. Dupasquier, I.J. Polmear, P. Folegati, R. Ferragut, Phys. Rev. B 61 (2000) 14454-14463.

[41]   A. Bharathi, C.S. Sundar, Mater. Sci. Forum. 105-110 (1992) 905-908.

[42]   J.R. Davis, Aluminum and Aluminum Alloys, ASM International, Materials Park, OH, 1998.

Figures
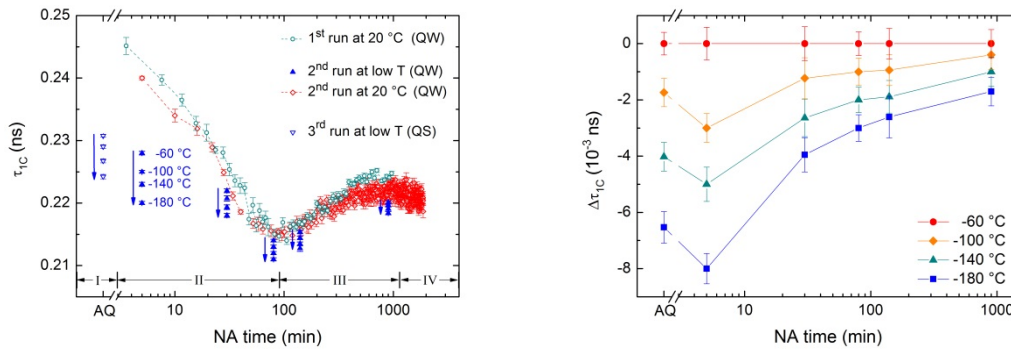
Fig. 1. **Evolution of one-component positron lifetime τ_{1C} during NA of Al-0.4Mg-0.4Si alloy**. (a) 1st run (green open circles): uninterrupted in-situ measurements starting directly after water quenching (QW). 2nd run (blue full triangles): low-temperature measurements at 4 different temperatures ($-60\,°C$, $-100\,°C$, $-140\,°C$, $-180\,°C$ in direction of arrow) carried out after previous NA for a time that can be read from the x-axis. During NA between the low-temperature measurements, τ_{1C} was measured continuously (red open diamonds). 'AQ' denotes a sample that was solid-state quenched (QS) in a 3rd run (blue open triangles) and was kept at low temperature throughout processing. At the bottom of the diagram, the four different stages of positron lifetime evolution are marked. (b) τ_{1C} data for the 4 different measurement temperatures in (a) presented as a difference to the values measured at $-60\,°C$.
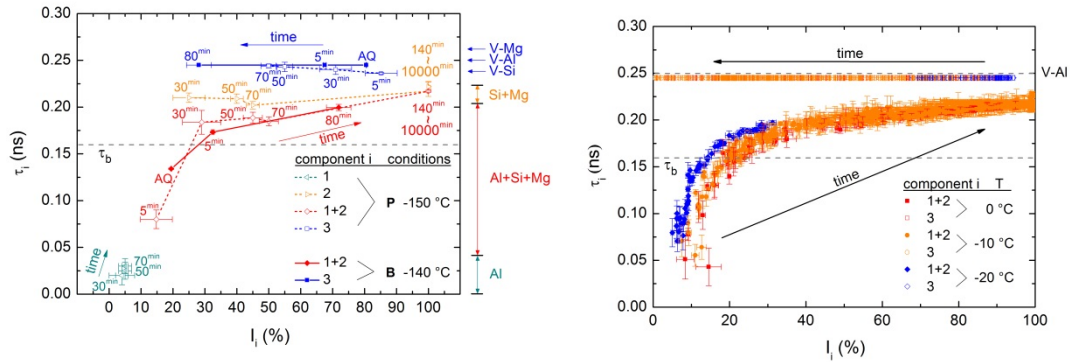
Fig. 2. **Positron lifetime components and corresponding intensities measured in alloy Al-0.4Mg-0.4Si after water quenching (QW) or solid states quenching (QW) and various NA times as specified by labels**. (a) Data measured in a cryostat at low temperature. Three-component fits obtained from data of spectrometer **P** are given by open symbols: bulk (1), solute cluster (2) and vacancy-related (3) component. Each τ_i is given as a function of corresponding I_i. In addition, components τ_1 and τ_2 have been summed up to a virtual component τ_{1+2}. 1½-component fits from data measured with spectrometer **B** are represented by full symbols: the fixed vacancy-related component τ_3 and the remaining component representing τ_{1+2}. On the right side of the graph typical values for a vacancy in Al, or V-Mg and V-Si complex in Al are given as well as the expected range for lifetimes in solute clusters [3], the reduced bulk lifetime and the mixture of both. (b) Data obtained with spectrometer **B** in-situ during ageing at three NA temperatures (0 °C, −10 °C, −20 °C). 1½-component fits with a fixed vacancy-related component τ_3 were performed. The arrow indicates increasing time which is an implicit parameter here.
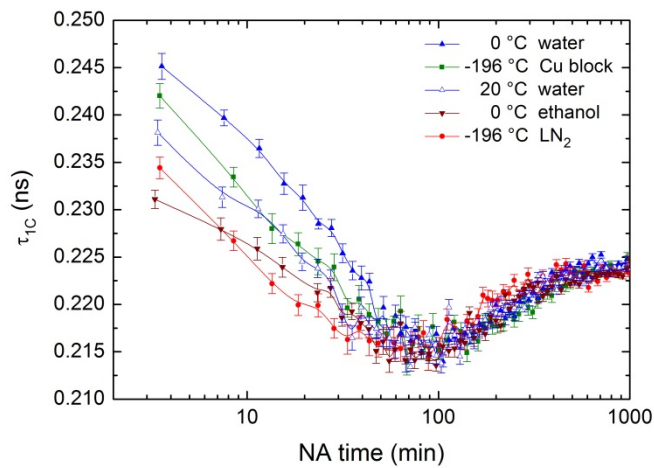
Fig. 3. **One-component positron lifetime in samples of alloy Al-0.4Mg-0.4Si during NA after quenching into various quenching media**.
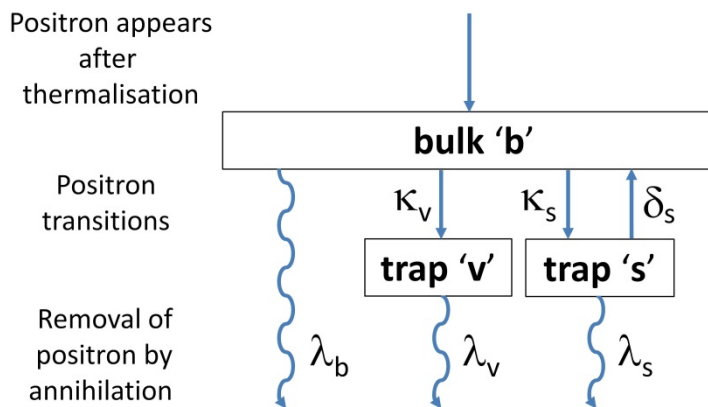
Fig. 4. **Schematic representation of three-state trapping model with one deep trap (vacancy-related defects 's') and one shallow trap (solute cluster 's')** [20].
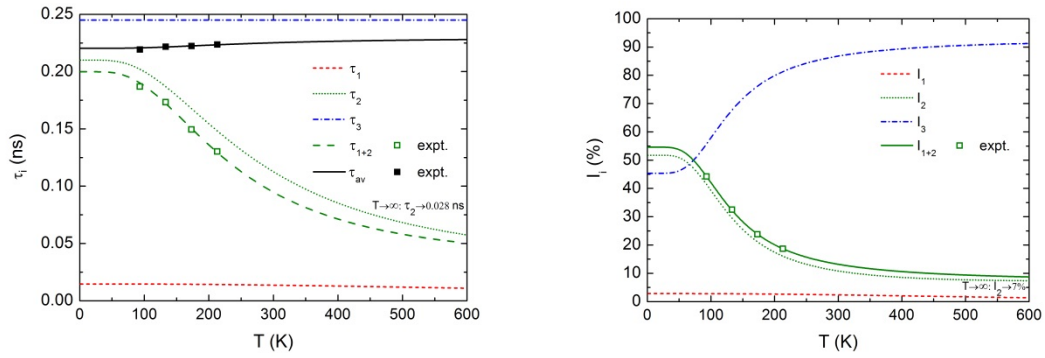
Fig. 5. **Temperature dependence of positron annihilation in the sample NA for 5 min after solutionising and quenching**. Application of the three-state trapping model with annihilation rates determined by least square fitting of the model to the experimental data. (a) Calculated positron lifetimes compared to experimental data, (b) Corresponding intensities.
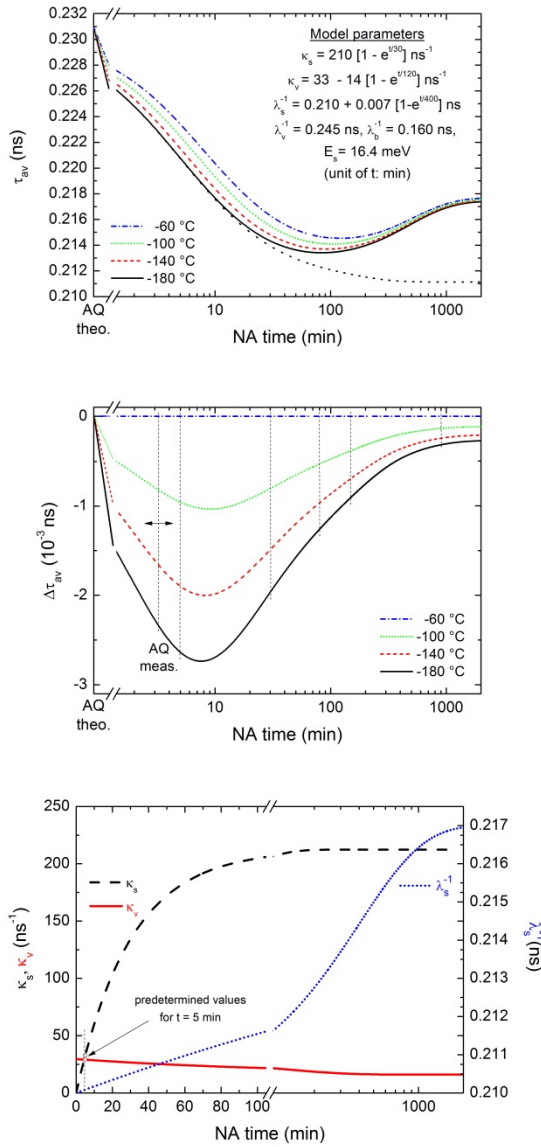
Fig. 6. **Calculation of the change of average positron lifetime τ_{av} during NA at different measurement temperatures (lower than the ageing temperature)**. (a) Absolute average positron lifetime for four measurement temperatures. For −180 °C, the broken curve corresponds to a constant value of λ_{s} ($\Delta\lambda_{s}$ = 0 in Eq. (11)), (b) Difference $\Delta\tau_{\mathrm{av}}$ to lifetime values calculated for −60 °C. (c) Change of trapping and annihilation rates during NA. The model parameters applied are given in (a).

κ_v (ns^{-1})	c_v (m^{-3} or atom^{-1})	κ_s (ns^{-1})	c_s (m^{-3} or atom^{-1})	E_s (meV)
29	7.2×10^{24} or 1.2×10^{-4}	33	2.4×10^{25} or 4×10^{-4}	16.4

Table 1. **Parameters derived for Al-0.4Mg-0.4Si alloy naturally aged for 5 min after quenching**. κ is the positron trapping rate of vacancy-related defects (v) or solute clusters (s), c the density of vacancies (v) or solute clusters (s), E_s the binding energy between a positron and a solute cluster.